Torsional coupling effects in the earthquake response of asymmetric buildings

A. M. Chandler

Department of Civil Engineering, King's College, London, UK

G. L. Hutchinson

Department of Civil and Agricultural Engineering, University of Melbourne, Melbourne, Victoria, Australia

(Received June 1985)

This paper presents a detailed parametric study of the coupled lateral and torsional response of a partially symmetric single storey building model subjected to both steady state and earthquake base loadings. It is shown that the qualitative effects of the controlling parameters on the maximum translational and torsional responses of the coupled system are not affected by the nature of the loading. The maximum lateral edge displacement of the building arising from the combined response effects is investigated. The related lateral shear forces in vertical resisting elements located on the periphery of the structure may be significantly increased in comparison with the corresponding values for a symmetric building. It is concluded that for particular ranges of the key parameters defining the structural system, typical of the properties of many actual buildings, torsional coupling induces a significant amplification of earthquake forces which should be accounted for in their design.

Key words: torsional coupling, earthquakes, asymmetric buildings, fast Fourier transform

Forced vibration tests on existing buildings[1–4] indicate that, in some cases, significant torsional effects are induced by the applied dynamic excitation. These effects are to be expected when buildings with their centre of mass significantly offset from their centre of resistance are subjected to horizontal translational ground motion, as in an earthquake, since the inertia forces acting at the centre of mass at each storey level and the resisting forces acting at the centres of resistance form a dynamic couple which interconnects the translational and torsional response of the building. Analytical investigations of dynamic torsional coupling[5–9] have concluded that its effects are most significant when the translational and torsional natural frequencies of the equivalent uncoupled building (with the eccentricity between the centres of mass and resistance neglected) are close, and that relatively large torsional motions may be generated under such circumstances even in buildings which are nominally symmetric.

Studies of multi-storey eccentric structures[5,10,11] have shown that torsional coupling can in many cases be predicted by a knowledge of the dynamic characteristics of equivalent single storey buildings, and hence the use of an idealized model with only two independent degrees of freedom, as in this study, is sufficient to identify the more significant trends in the earthquake response of torsionally coupled systems. Previous parametric investigations of idealized single storey building systems[6–9,12,13] have generated design procedures accounting for coupling effects which have been imple-

0141-0296/86/04222-15/$03.00

mented in all the major building codes in the form of expressions defining an equivalent static design torque.[14–16] Such investigations make widespread use of idealized response spectra to characterize the earthquake ground motion. Such so-called design spectra are obtained by averaging and smoothing the distribution of responses to several earthquake records, preferably from the local region. Bearing in mind their idealized nature, and the difficulties encountered in achieving accurate procedures for combining the modal maxima,[17] a number of current earthquake codes[18,19] recommend that the user of design spectra should check results by performing one or more time-history analyses using earthquake records obtained from the region of interest. The ability of the designer to perform these calculations in individual cases will depend on the availability of suitable local records. Recent research[20,21] has, however, enabled the problem of record availability to be avoided in some cases by the generation of simulated earthquake records possessing the primary characteristics of earthquakes in a particular region.

The use of artificially generated records is still at an early stage of development and greater understanding of earthquake properties as they affect engineering structures, and in particular their relative importance, is required to enable confident use of artificial accelerograms in a design situation.

The widespread use of response or design spectra in research studies, particularly those which are parametric in nature,[22,23] is due primarily to their convenience and simplicity. Errors may arise, however, in their application to the analysis of multi degree of freedom systems, especially if subjected to earthquakes of a realistic, multi-component form. In some cases, the results obtained in the analysis of earthquake response using response spectra have been compared with limited time history response studies[23] which have emphasized that under some circumstances, responses obtained by the latter approach may significantly exceed those obtained using idealized spectra. This is primarily because the frequency content of any real earthquake, and hence the degree to which it will excite the response of structures with particular natural frequencies, is randomly variable whereas a smoothed spectrum has, by definition, removed the individual peaks and troughs leaving only the overall trend. This modification will clearly affect the maximum response of a particular structure to an individual earthquake although it may be argued, with some justification, that the non-repeatability of an earthquake and its associated detailed spectral pattern justifies the averaging and smoothing operations employed. The use of design spectra, in which these operations are incorporated at the outset of the analysis, therefore provides the most convenient tool for earthquake response calculations, especially for the designer who will wish to minimize the computational effort in dynamic analysis. The need is still apparent, however, for researchers to increase the use of time history analysis in an attempt to substantiate, and confirm, the parametric response trends identified by other more simplified analyses.

The work presented in this paper comprises the first stage of a systematic effort to assess, parametrically, the influence of torsional coupling on the elastic earthquake response of buildings subjected to transient earthquake records. In the first instance, a brief study is made of the responses to steady state harmonic base loading, both to examine maximum response trends and to develop response functions for subsequent incorporation into an analysis of transient response by frequency domain methods.

Description of the system

Building model

The single storey building model to be analysed is shown in *Figure 1(a)*. The floor diaphragm is assumed to be an infinitely rigid circular disc of radius r and the total mass of the building is represented by the mass m of the disc. A circular floor plan is chosen to enable straightforward extension of these studies to an analysis of the earthquake response of equivalent flexibly-based buildings.[24] The response displacements (translational and rotational) of the floor diaphragm are assumed to be sufficiently small to ensure the structural stability, and, therefore, the effects of changes in the geometry may be neglected.

The vertical elements are taken to be axially inextensible, and their combined lateral and torsional interstorey stiffnesses are idealized by massless, elastic and viscously damped springs (*Figure 1(c)*). Furthermore, a symmetrical distribution of the lateral stiffness is assumed, such that the centre of resistance coincides with the centre of the disc. The structural eccentricity e, between the centres of mass and resistance and perpendicular to the loading direction x, is caused by different mass densities (ρ_a, ρ_b; $\rho_a > \rho_b$) in the two halves of the floor disc, split along $y = 0$, as shown in *Figure 1(b)*. Thus the range of values[24] of e is $0 \leqslant e \leqslant 4r/3\pi$. The principal axes of resistance coincide with the x and y horizontal axes of the reference system, and hence, rotational displacements θ of the disc take place about the centre of resistance ($x = y = 0$).

Steady state ground motion input

For the purposes of establishing the frequency domain solution to the equations of motion, the ground excitation is assumed to be applied as a harmonic, rigid-base displacement v_g in the x-direction (perpendicular to the eccentricity):

$$v_g = \bar{v}_g \exp(i\omega t) \tag{1}$$

where ω is the circular frequency of excitation and $\bar{v}_g$ is the ground displacement amplitude.

Analytical solution of the equations of motion

The equations of motion of the building model (*Figure 1*) are derived from the expression of dynamic equilibrium for each degree of freedom:

$$m\ddot{v}^t + me\ddot{\theta} + c_{vv}\dot{v} + c_{v\theta}\dot{\theta} + K_v v = 0 \tag{2}$$

$$me\ddot{v}^t + J_\theta\ddot{\theta} + c_{\theta v}\dot{v} + c_{\theta\theta}\dot{\theta} + K_\theta\theta = 0 \tag{3}$$

where v^t is the total translational displacement of the floor mass in the x-direction, i.e. $v^t = v_g + v$; θ is the rotational displacement of the floor mass about the z-axis; K_v and K_θ are the translational and torsional storey stiffness, respectively; c_{vv}, $c_{\theta\theta}$ and $c_{v\theta}$ ($=c_{\theta v}$) are viscous damping coefficients; J_θ is the mass polar moment of inertia about the centre of resistance; and e is the static eccentricity.

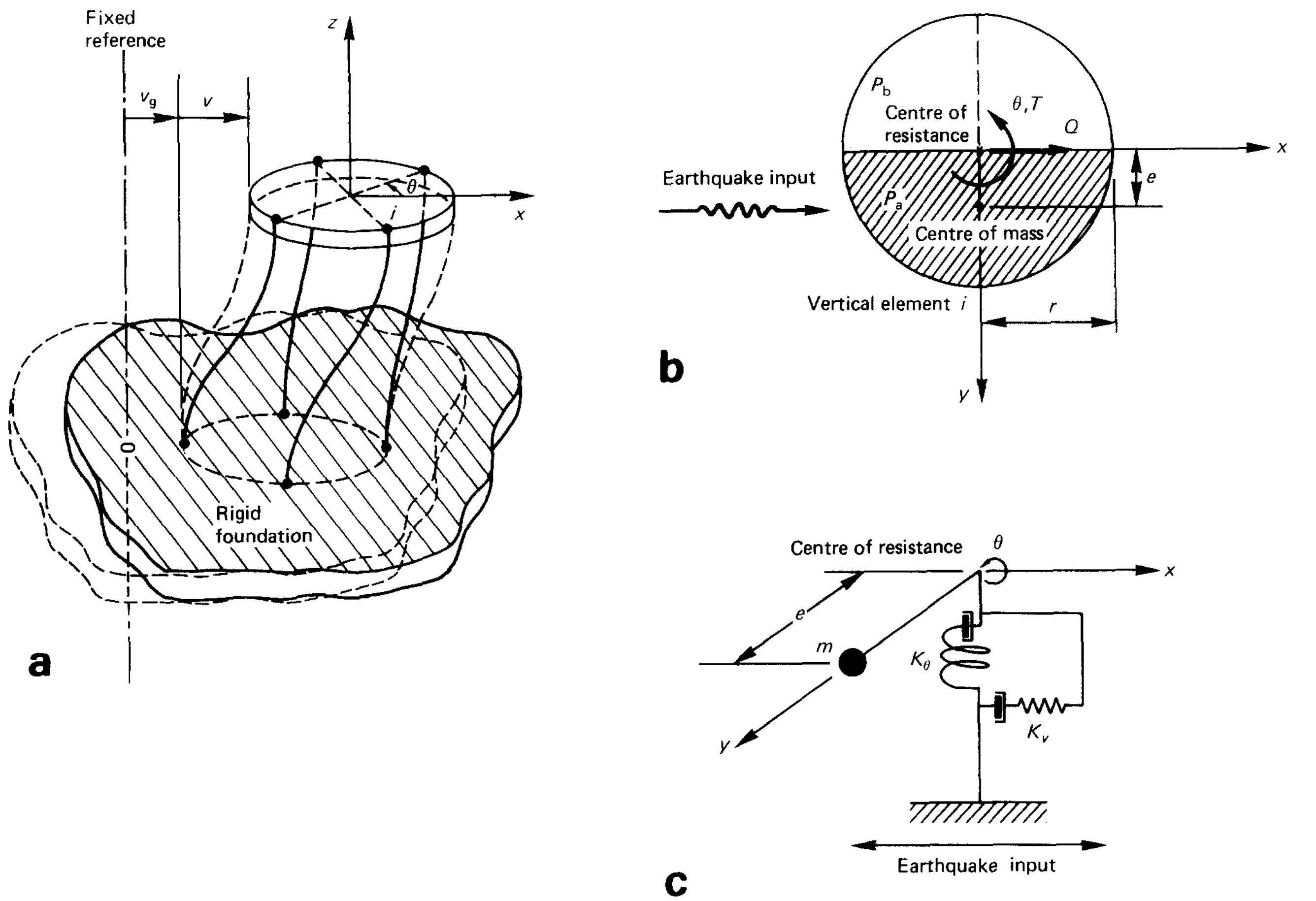

Figure 1 Torsionally coupled single storey building model: (a) response under rigid base ground excitation; (b) typical plan view of floor diaphragm; (c) corresponding mathematical model

The equations of motion may be expressed in parametric form as:

$$\ddot{v}^t + e_r\ddot{v}_\theta + 2\xi\omega_1 D_{vv}\dot{v} + 2\xi\omega_1 e_r D_{v\theta}\dot{v}_\theta + (\omega_1^2/\Omega_1^2)v = 0 \quad (4)$$

$$e_r\ddot{v}^t + 0.5\,\ddot{v}_\theta + 2\xi\omega_1 e_r D_{v\theta}\dot{v} + \xi\omega_1 D_{\theta\theta}\dot{v}_\theta + 0.5\,(\omega_1^2/\Omega_1^2)\,\lambda_T^2 v_\theta = 0 \quad (5)$$

where $v_\theta = r\theta$; $e_r = e/r$; ω_1 is the fundamental coupled natural frequency of the building; $\Omega_1 = \omega_1/\omega_v$ where ω_v is the translational natural frequency of the torsionally uncoupled building ($e = 0$), i.e. $\omega_v = [(K_v/m)]^{\frac{1}{2}}$; $\lambda_T = \omega_\theta/\omega_v$ where ω_θ is the torsional natural frequency of the uncoupled building, i.e. $\omega_\theta = [(K_\theta/J_\theta)]^{\frac{1}{2}}$; D_{vv}, $D_{v\theta}$, $D_{\theta\theta}$ are dimensionless damping coefficients determined by assuming that the building has normal modes with equal viscous damping ratio ξ. (For the calculation of D_{vv}, $D_{v\theta}$, $D_{\theta\theta}$, see reference 24.)

For harmonic ground displacement in the form given in equation (1), the steady state responses of the building at frequency ω are expressed in terms of complex frequency response (transfer) functions H_v and H_θ where, for the linear system under consideration, $v = H_v \exp(i\omega t)$ and $v_\theta = H_\theta \exp(i\omega t)$. Substituting these expressions in equations (4) and (5) yields the following pair of linear algebraic equations with complex coefficients:

$$(1/\Omega_1^2 - f^2 + 2i\xi f D_{vv})H_v/\bar{v}_g + e_r(-f^2 + 2i\xi f D_{v\theta})H_\theta/\bar{v}_g = f^2 \quad (6)$$

$$e_r(-f^2 + 2i\xi f D_{v\theta})H_v/\bar{v}_g + (0.5\,\lambda_T^2/\Omega_1^2 - 0.5f^2 + i\xi f D_{\theta\theta})H_\theta/\bar{v}_g = e_r f^2 \quad (7)$$

where f is the excitation frequency ratio, i.e. $f = \omega/\omega_1$. The solution of equations (6) and (7) yields the complex frequency response functions H_v and H_θ, normalized with respect to the amplitude, $\bar{v}_g$, of the ground displacement. The response functions $H_v/\bar{v}_g$ and $H_\theta/\bar{v}_g$ depend only on the parameters e_r, λ_T, ξ and f, where the first three quantities define the structural system and the latter, together with the amplitude $\bar{v}_g$, defines the ground motion.

Steady state effects of torsional coupling

The coupled natural frequency ratios $\Omega_n = \omega_n/\omega_v$, for $n = 1, 2$, are plotted in *Figure 2* as a function of the parameters λ_T and e_r, termed the uncoupled frequency ratio and static eccentricity ratio, respectively. It is shown that for λ_T close to unity, and for small eccentricities, the modal natural frequencies of the system ω_1 and ω_2 are close to the translational natural frequency ω_v of the uncoupled (single degree of freedom) system. Under these conditions, strong modal coupling may occur, as observed by several previous investigators.[1,6,22,25] For large eccentricities and/or values of λ_T other than unity, the modal frequencies are well separated and, hence, coupling effects are expected to be less evident. Furthermore, it may be concluded that the presence of close uncoupled torsional and translational

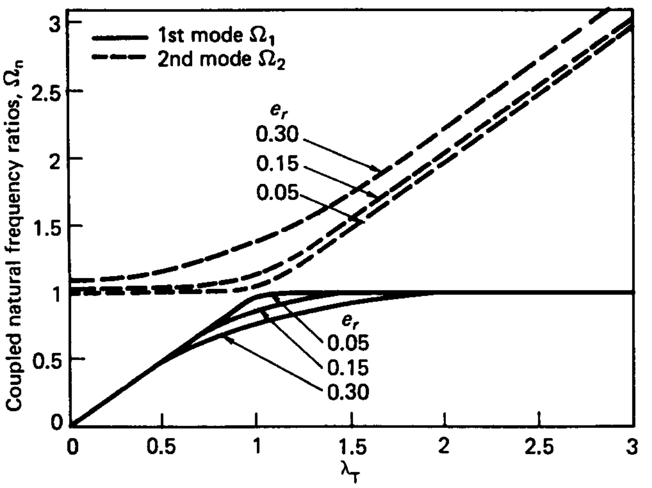

Figure 2 Effects of parameters λ_T and e_r on natural frequencies of torsionally coupled building

natural frequencies ($\lambda_T \simeq 1$) is, in itself, not a sufficient condition for significant torsional coupling to occur since the actual, coupled natural frequencies are widely separated at large eccentricities, even at $\lambda_T = 1$. These results confirm those obtained in an earlier investigation[22] using an equivalent single storey building model, and they are also in agreement with the observations of Tso and Meng[25] in a study of the earthquake responses of torsionally coupled multistorey buildings, both investigations using idealized response spectra to represent the earthquake input.

The parametric response trends exhibited by the translational and torsional components of response are investigated in *Figures 3* and *4*, which show the frequency response characteristics (amplitude and phase) for a building with moderate eccentricity ($e_r = 0.15$) and assuming modal damping to be 5% of critical damping. At high excitation frequencies, the amplitude $\bar{v}$ tends to be equal to the amplitude of the ground displacement, $\bar{v}_g$, whereas the amplitude $\bar{v}_\theta$ becomes zero. For values of λ_T other than unity, the natural frequencies of the system are well separated, and, therefore, the response amplitudes exhibit two distinct peaks. *Figure 3(a)* shows that, for $\lambda_T < 1$, the first resonant amplitude (at $\omega = \omega_1$ and $f = 1$) of the translational displacement, $\bar{v}$, is significantly smaller than the second resonant amplitude (at $\omega = \omega_2$ and $f = \omega_2/\omega_1$). This is because, for $\lambda_T < 1$, the first vibration mode of the system is mainly torsional, thus contributing very little to the translational response of the system. Conversely, in the case of $\lambda_T > 1$ the first resonance of $\bar{v}$ is more severe when compared with the second resonance.

Figures 3(b) and *4(b)* show the variation of the response phase angles ψ_v and ψ_θ with excitation frequency. The nature of the complex component of the torsional response function H_θ is such that phase angles occur over the range $0 < \psi_\theta < 360°$, whilst the translational response has phase angles limited to the range $0 < \psi_v < 180°$. At low excitation frequencies, both the translational and torsional responses are almost in phase with the applied excitation, whilst at high frequencies, the translational response and torsional response have phase angles tending to 180° (out of phase) and 360° (in phase), respectively. The significance of phase effects is shown when considering the combined translational and torsional response of the system. This is investigated

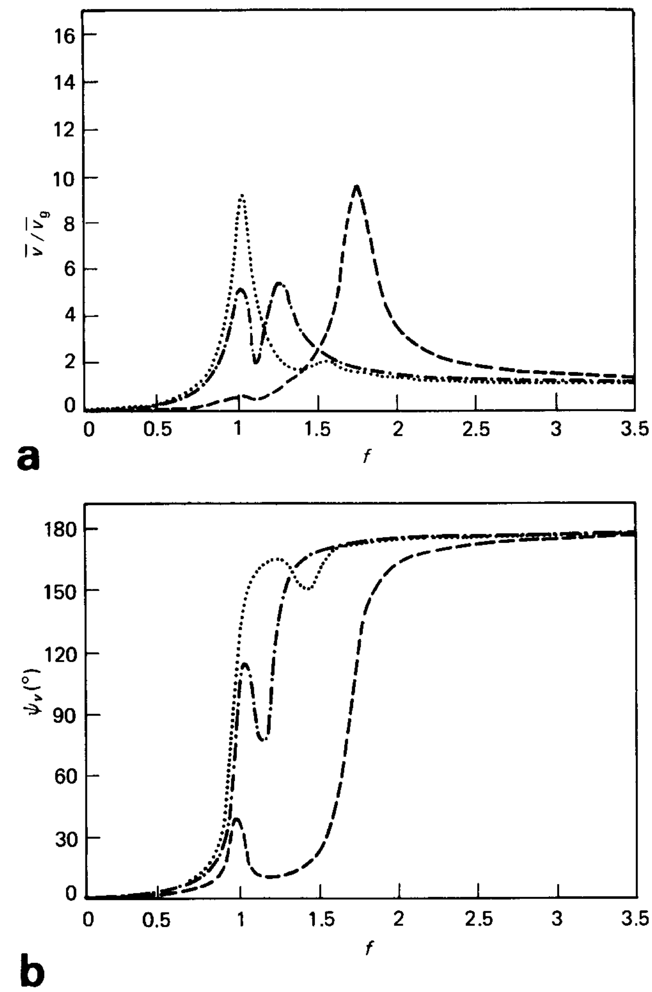

Figure 3 Translational displacement v of floor disc for various values of λ_T ($e_r = 0.15$): (– – – –) $\lambda_T = 0.6$; (– · – · – · –) $\lambda_T = 1$; (· · · ·) $\lambda_T = 1.4$; (a) amplitude; (b) phase angle

using a third response parameter $v_i = v + v_\theta$, where v_i represents the x-translation of a vertical element i located on the periphery of the disc at a distance r from the x-axis (*Figures 1(a)* and *(b)*). When the structure is subjected to earthquake loadings, the lateral displacement of element i is a quantity related to the primary design torque requirements as stipulated in the various building codes. The response v_i, which contains both amplitude and phase information from the individual translational and torsional response components v and v_θ is therefore, of importance in assessing the influence of torsional coupling in the chosen building model. The combined response amplitude, shown in *Figure 5(a)*, has a peak value which is significantly greater than the individual translational and torsional response peaks. The combined response is strongly influenced by the value of λ_T, with the greatest amplitudes occurring at the fundamental resonant frequency and for λ_T equal to, or greater than unity. The corresponding phase angle ψ_i is plotted in *Figure 5(b)*.

A direct comparison between torsional coupling effects in steady state and earthquake response (the latter obtained in earlier studies[5,22] using idealized response spectra) is achieved by plotting the maximum amplitudes of the response quantities v, v_θ and v_i against λ_T, as in *Figures 6(a)–(c)*. *Figure 6(a)* shows that for λ_T close to unity there is a reduction in the value of

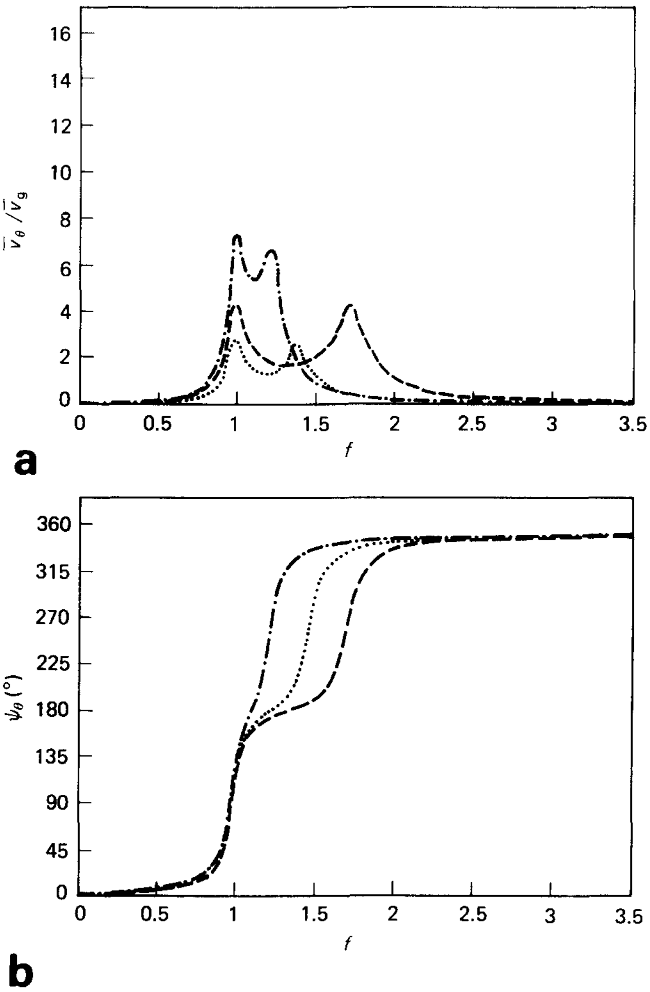

Figure 4 Torsional displacement v_θ of floor disc for various values of λ_T (e_r = 0.15): (– – – –) λ_T = 0.6; (–·–·–·–) λ_T = 1; (····) λ_T = 1.4; (a) amplitude; (b) phase angle

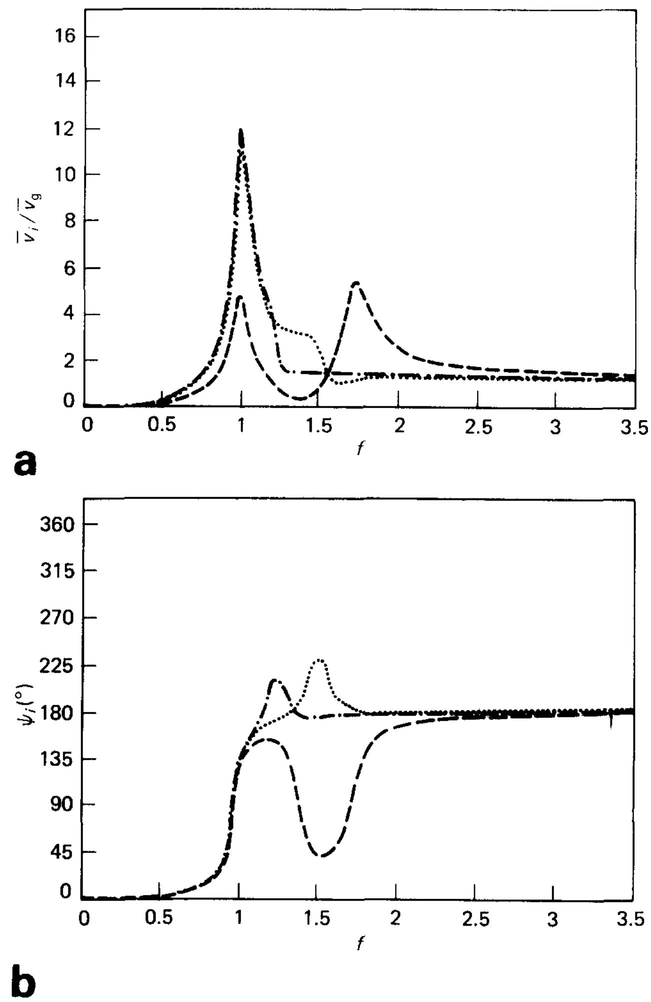

Figure 5 Combined displacement v_i of element i at edge of floor disc for various values of λ_T (e_r = 0.15): (– – – –) λ_T = 0.6; (–·–·–·–) λ_T = 1; (····) λ_T = 1.4; (a) amplitude; (b) phase angle

max $\bar{v}$, and this becomes more pronounced as the eccentricity increases. For the same range of values of λ_T, however, a significant increase of max $\bar{v}_\theta$ occurs, even for very small values of eccentricity (*Figure 6(b)*). In general, torsional coupling effects become negligible for values of λ_T greater than 2. These results indicate that there is a consistency among the parametric trends of torsional coupling developed in steady state and earthquake response. The variation of maximum values of the combined response $\bar{v}_i$ with λ_T is shown in *Figure 6(c)*, with the greatest values occurring when λ_T is somewhat greater than unity, for which the response is 25–30% greater than that obtained for the equivalent uncoupled system (e_r = 0). For λ_T less than about 0.8, the combined response amplitude $\bar{v}_i$ is less than that of the uncoupled system. This is because the phasing of the translational and torsional response is such as to produce some cancellation of edge displacement effects at this location and for this range of λ_T. It should be noted that most buildings will have frequency ratios λ_T in the range[25] $0.5 < \lambda_T < 1.5$ and that values less than 0.5 are very unlikely to occur.

In a design context, therefore, the maximum value of the edge displacement v_i will depend fundamentally on the value of λ_T. The results presented here indicate that the application of the primary torsional design requirement of the building codes, which is used in the calculation of the design lateral force on a typical edge element i, will be the most critical when $\lambda_T > 1.2$. For $\lambda_T < 0.8$, the maximum edge displacement is significantly reduced compared with that produced in the equivalent symmetric building, and, hence, a design based only on the design lateral shear force (or displacement) for the symmetric case would yield conservative results for the coupled system in this range of λ_T. For values of λ_T in the intermediate range $0.8 < \lambda_T < 1.2$ (typical of many real buildings), the choice of the appropriate design provision will depend largely on the magnitude of the eccentricity ratio e_r. It is in this critical latter range of λ_T, in particular, that further studies of coupling effects under realistic earthquake loadings are required. The remainder of this study is aimed at achieving greater understanding in these areas, based primarily upon a confirmation of the response trends identified in this preliminary study of steady state torsional coupling effects.

Classification of earthquake records for response analysis

The primary purpose of this study is to assess torsional coupling effects in asymmetric buildings under actual earthquake excitations using frequency domain analyses. In addition to their use in response analysis, earthquake response spectra provide a useful means for assessing the engineering significance of an earthquake

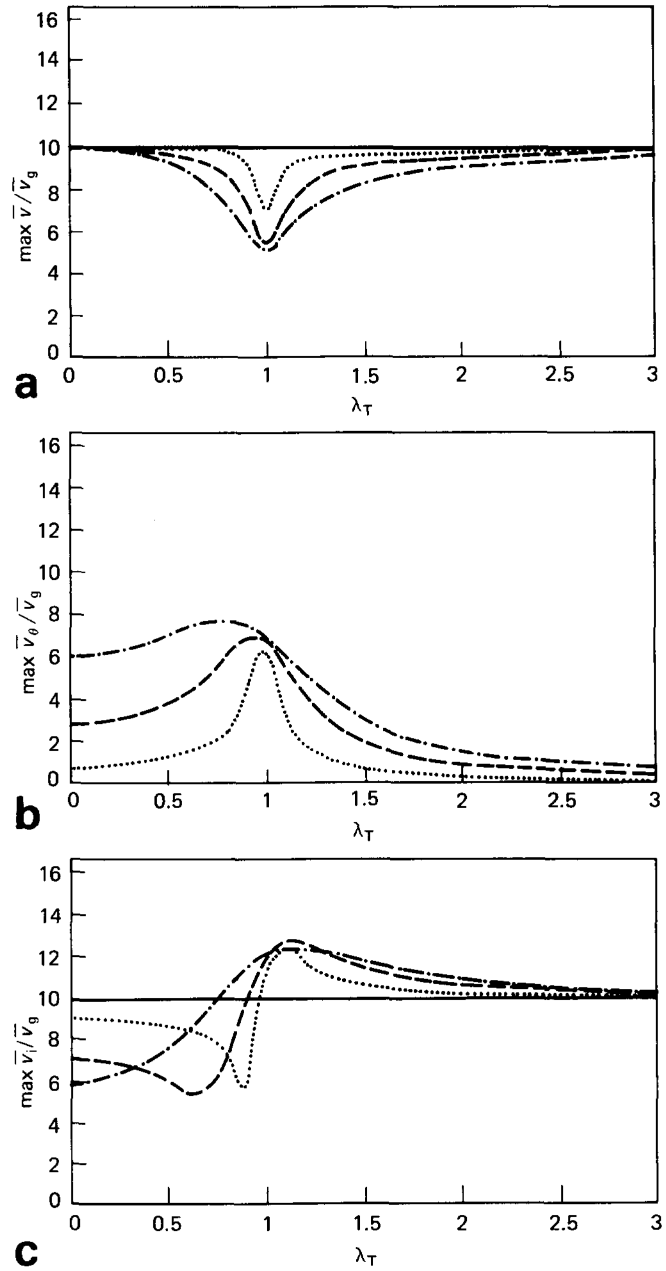

Figure 6 Variation of maximum amplitudes of displacement responses of floor disc with λ_T: (——) $e_r = 0$; (····) $e_r = 0.05$; (- - - -) $e_r = 0.15$; (-·-·-·-) $e_r = 0.3$; (a) v; (b) v_θ; (c) v_i

in terms of the response of a simple single degree of freedom (SDOF) system. The Fourier amplitude spectrum can be employed in a similar way to yield information concerning the frequency content of an earthquake acceleration record. In the design of earthquake-resistant structures, for example, the severity (or magnitude) of the vibratory motion is represented primarily by the magnitude of the response spectrum, whereas the frequency content and to some extent the soil characteristics are specified by the fundamental shape of both the response and Fourier spectra. It is well established that response spectra obtained from strong-motion earthquakes recorded in different parts of the world do not exhibit the same characteristics.[26,27] The properties of response spectra depend, for example, on the location within the earthquake zone and on the prevailing geological conditions. The selection of appropriate localized response spectra, and the variation of their effect upon the earthquake response of low-rise structures, has been studied in a previous work.[27]

The ground motions employed in the analysis of torsionally coupled structures with one eccentricity component (*Figure 1*) are chosen, with one exception, from recent strong-motion European earthquake records. A total of eight records have been employed; the digitized acceleration records, corrected using the parabolic baseline correction technique,[28] are plotted in *Figure 7*. A complete set of integrated velocity and displacement time histories for the records used is given in reference 29. The selected European earthquake motions are chosen from countries which share a common geographical area, although a study of their spectra[29] indicates that the mechanism by which they arose, and the effect of local soil conditions, is significant in establishing a suitable classification system for the recorded surface accelerations.

Figure 7 shows the Romanian earthquake of 1977, together with the Greek earthquakes of 1973 (Leukas), 1974 (Patras) and 1978 (Thessaloniki), and three separate recordings from the Italian earthquake of 1972 (Ancona–Rocca). Also shown in *Figure 7* is the 1940 El Centro (California) earthquake record. This latter record has been widely used in earthquake response analyses, and represents one of the most severe combinations of strong motion ground acceleration over long duration amongst existing records. For these reasons, the El Centro record has been included in order to provide a comparison with the responses to the selected European earthquakes.

The Fourier amplitude spectra of the eight selected earthquake records[27,29] are used to describe their frequency content, which will give a valuable indication of the types of structure (designated by their fundamental natural frequency) likely to be most severely damaged. In earthquakes whose dominant frequencies are limited to a relatively narrow band, in particular where local soil conditions have resulted in severe amplification at certain critical frequencies (usually in the low frequency range), the resulting damage is confined largely to those buildings whose natural frequencies lie within the dominant band. Examples of this category are the Romanian earthquake of 1977, and the Greek earthquakes of 1973 (Leukas) and 1978 (Thessaloniki). The effect is particularly noticeable for the Romanian earthquake, where much of the total energy is concentrated at frequencies less than 1.25 Hz. A reconnaissance report[30] published soon after the earthquake indicated that by far the greatest structural damage in the Romanian capital Bucharest was suffered by relatively light, reinforced concrete buildings 8–14 storeys high, with natural frequencies between 0.7 and 1.2 Hz. This observation confirms the indications given by the Fourier spectrum of the earthquake record. It was also noted that the relatively high stiffness of the massive reinforced concrete structures, generally six to eight storeys high, which are typical of post-war construction in the region, resulted in relatively high fundamental frequencies of vibration and hence these buildings survived the earthquake with little or no damage.

A different form is observed in the spectral shape of the Greek earthquake of 1974 (Patras) and the set of Italian earthquake records of 1972 (Ancona–Rocca). The distribution of energy for these earthquakes is more uniform, with significant amplitudes occurring over a

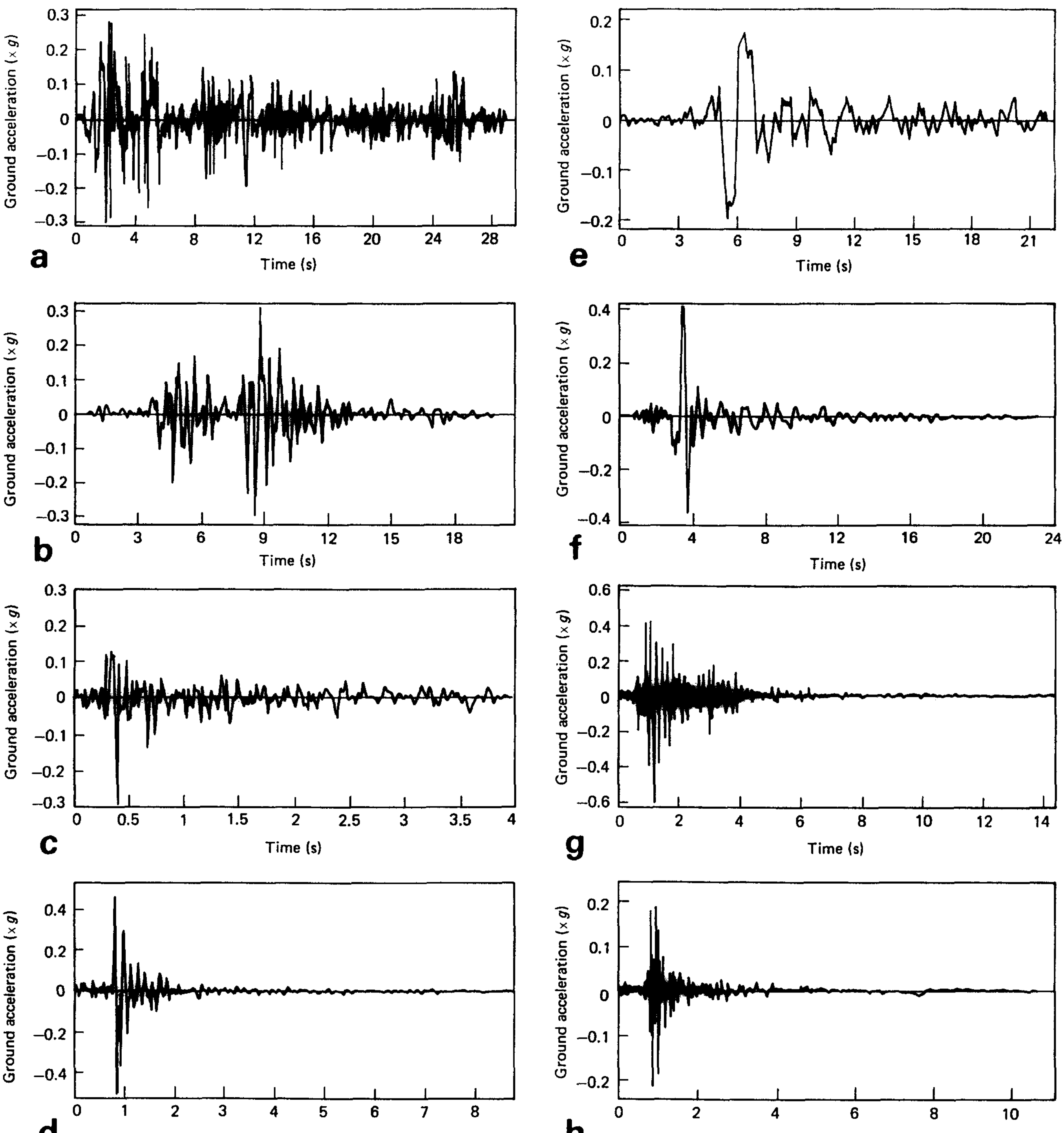

Figure 7 Corrected earthquake accelerogram records: (a) El Centro, 18 May 1940, N-S component; (b) Thessaloniki, 20 June 1978, horizontal A; (c) Patras, 29 January 1974, transverse component; (d) Ancona–Rocca, 14 June 1972, 23:01, T16 N-S component; (e) Romania, 4 March 1977, N-S component; (f) Leukas, November 1973, longitudinal component; (g) Ancona–Rocca, 14 June 1972, 20:56, T15 N-S component; (h) Ancona–Rocca, 21 June 1972, 17:06, T18 N-S component

much wider range of frequencies. The prediction of damage effects due to earthquakes of this type is more complex, and the damage itself likely to be more widespread because of the broader range of building types affected. In general, earthquakes in the second category are likely to affect structures in the high frequency range more severely, and those in the low frequency range less severely, than those in the first category.

The similarity in the spectral shape evident in certain of the European earthquakes classifies them as comparable spectra for the purpose of earthquake response analysis. Studying the Fourier amplitude spectra from the individual earthquakes, two separate categories of input motions have been identified:[27,29]

(A) a 'peaking' spectrum, exhibiting dominant frequencies over a well-defined range; the Romanian, Leukas and Thessaloniki earthquake records are examples of this category

(B) a 'broad-band' spectrum, with approximately uniform amplitudes (that is, no distinct bands of dominant frequencies) over the relevant frequency range; the Patras and Ancona–Rocca earthquake records are in this category

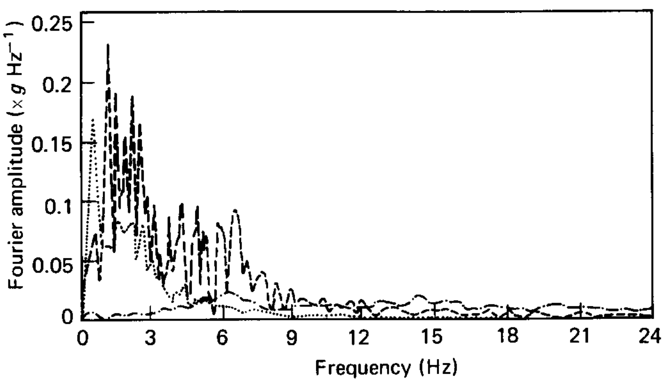

Figure 8 Normalized and averaged Fourier amplitude spectra: (– – – –) N–S El Centro; (····) European set A; (–·–·–·–) European set B

These two sets of comparable spectra are henceforward classified European set A and European set B, respectively. In *Figure 8*, the normalized and averaged Fourier amplitude spectra corresponding to these two sets of earthquakes, together with the corresponding El Centro spectrum, are illustrated for comparison. The individual ground acceleration records have been normalized to a peak value of $0.30g$ prior to calculating their spectra. The graphs indicate that in the low frequency range (<1 Hz), the European set A earthquakes dominate, whereas at high frequencies (>12 Hz) the European set B earthquakes have the greatest amplitudes, although in this range the amplitudes are in all cases relatively small. The El Centro earthquake, in the low frequency range (<3 Hz), has spectral characteristics which are similar to the European set A earthquakes. For frequencies in the range 3–8 Hz, however, the El Centro record shows significantly greater amplitudes than the European earthquakes, partly due to the abnormally long duration of severe shaking present in the El Centro record (around 29 s), compared with that of the Leukas and Thessaloniki earthquakes (around 10 and 12 s, respectively, see *Figure 7*). Some account should also be taken of the smoothing effect which has been brought about in averaging the European spectra (sets A and B).

In addition to a study of the frequency content of the chosen earthquake records, it is also of value to compute the associated response spectra. These are calculated by frequency domain analyses using the fast Fourier transform (FFT) technique.[31,32] The spectral acceleration curves shown in *Figure 9* are normalized to $0.30g$ peak ground acceleration and, for the European earthquakes, are averaged within categories A and B. The trends exhibited by the three sets of spectral response curves give further weight to earlier observations.

The El Centro record excites a consistently high level of normalized response for low periods, in the range $0.1 < T_v < 0.5$ s, corresponding approximately to the fundamental period of low-rise structures one to five storeys high. For a high damping value of 20%, within this period range, the spectral acceleration is nearly constant at around $0.5g$, representing an amplification of 60–70% compared with the normalized peak ground acceleration. For periods higher than 0.5 s, the response curves fall off rapidly to values around $0.1–0.2g$ at the cut-off period of 2 s, corresponding approximately to the fundamental period of a 20 storey building of steel-framed construction.

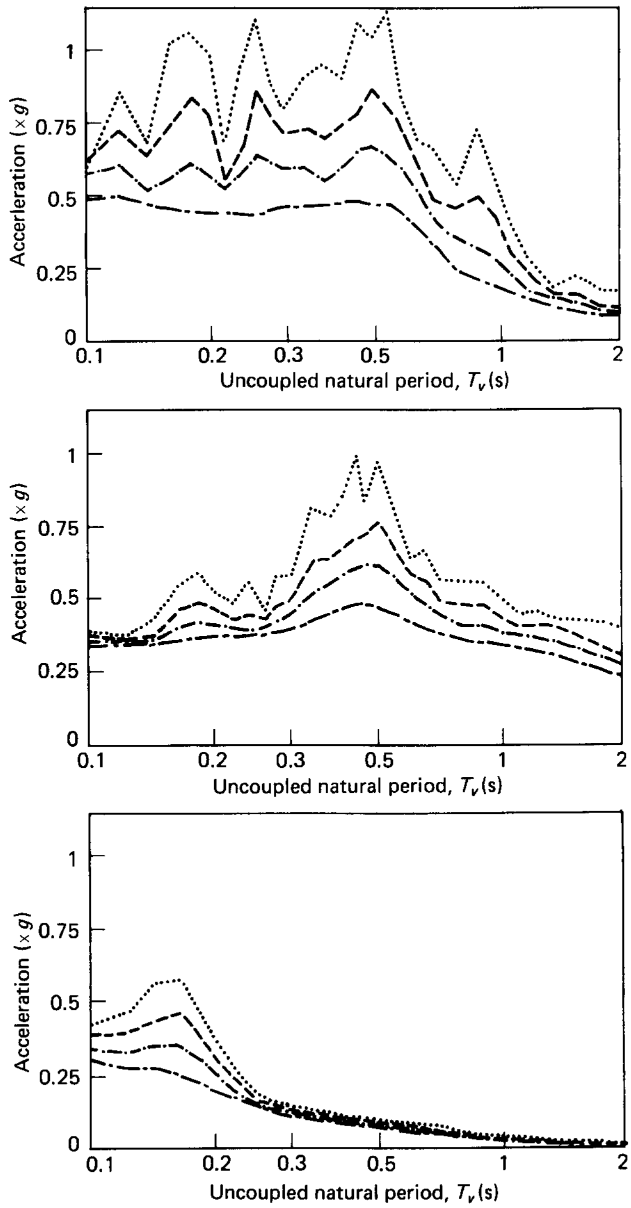

Figure 9 Normalized and averaged acceleration response spectra: (a) N–S El Centro; (b) European set A; (c) European set B; (····) $\xi = 0.02$; (– – – –) $\xi = 0.05$; (–·–·–·–) $\xi = 0.1$; (— — —) $\xi = 0.2$

The shape of the spectral curves for the El Centro earthquake, particularly noticeable at higher damping values whose effect is to produce a somewhat smoothed response curve, is typical of the flat-hyperbolic idealization commonly employed in the derivation of design spectra. The spectral curves for the European set A earthquakes (shown in *Figure 9(b)*) emphasize the observations made earlier; the largest spectral response values occur in the range 0.3–1 s, and peak at around 0.45–0.5 s. The most significant difference between the European set A and El Centro spectra occurs in the low period range (<0.3 s) where responses due to the European earthquakes are, on average, 30–40% smaller. The converse is true for periods greater than 1 s, where the fall-off in response values is less rapid for the European set A earthquakes.

Such a spectral shape is typical of many European earthquakes, especially those which occur in regions

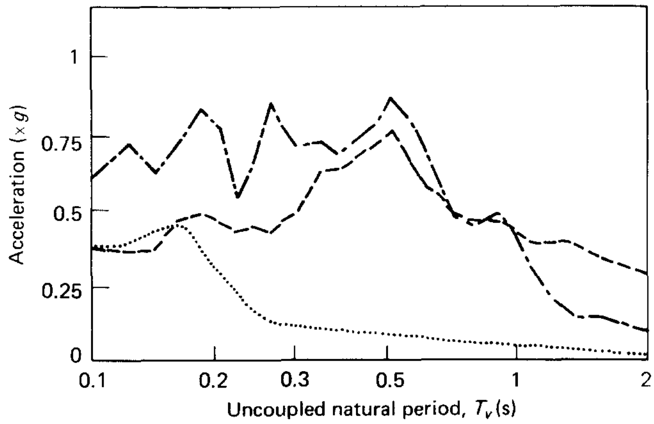

Figure 10 Normalized and averaged aceleration response spectra: (— — —) N-S El Centro; (- - - -) European set A; (····) European set B; $\xi = 0.05$

where the presence of soft soil deposits overlying deep gravel or dense sand layers causes amplification of the base rock acceleration, especially at longer periods. The resultant spectral curves are, however, quite unusual when compared with the 'standard' design spectra assumed in many parts of the world. The normalized spectral curves for the European set B earthquakes (*Figure 9(c)*) show predominant values for the very low period range (0.1–0.25 s), with rapid fall-off to very small response values at higher periods. These earthquakes are likely to induce significant damage in low-rise buildings up to three or four storeys, with negligible effect on taller structures. Finally, for comparative purposes, the spectral curves for 5% damping are shown in *Figure 10* for the El Centro, European set A and set B earthquakes.

Torsional coupling effects in earthquake response

In the analysis of earthquake response, it is assumed that a uni-directional earthquake ground acceleration input, $\ddot{v}_g(t)$, is applied uniformly over the base of the structure illustrated in *Figure 1*. The structure is supported on a rigid foundation, hence interaction effects have been neglected. Each of the responses v, v_θ and v_i, identified earlier, is evaluated in terms of time history displacement or absolute acceleration records, for a particular earthquake excitation. The calculation is carried out in the frequency domain employing the FFT technique[32] to evaluate the transient responses. The complex frequency response functions H_v, H_θ and H_i ($=H_v + H_\theta$) are evaluated in discrete form from the solution of equations (6) and (7). The derived earthquake responses depend on the structural parameters e_r, λ_T and ξ, as previously defined, together with the translational natural period T_v of the corresponding uncoupled model, as well as the earthquake record itself. The damping ratio ξ will henceforth be taken as 5% of critical damping, i.e. $\xi = 0.05$.

Figure 11 illustrates the time history displacement responses in the translational, torsional and combined modes, for a system with $e_r = 0.10$, $\lambda_T = 1$ and $T_v = 0.5$ s, subjected to the N-S El Centro earthquake record. The peak responses, circled, occur almost simultaneously at around 2.5 s (translational), 2.95 s (torsional) and 2.4 s (combined) following the commencement of the earthquake, which is of duration 29 s. The peak responses are, respectively, 5 cm, 4.1 cm and 6.7 cm. For the same earthquake, the maximum translational response of the corresponding uncoupled system ($e_r = 0$, $T_v = 0.5$ s, $\xi = 0.05$) is 5.6 cm. Hence, the effects of torsional coupling on the responses of this system with relatively small eccentricity are to reduce the maximum translational response at the centre of resistance (CR) by 11%, whilst increasing the maximum lateral displacement of the edge element i by 20% as a result of the induced rotational response about CR. These comments are in qualitative agreement with the effects observed under steady-state loading as described earlier. A reduction in shear of 36% and an increase in edge displacement of 19% are observed from *Figures 6(a)* and *6(c)*, for the same system. Hence, although the reduction in maximum shear due to torsional coupling under steady state loading is more than three times the calculated value under the El Centro earthquake loading, there is very good agreement between the respective amplification values for edge displacements.

It should be noted that the combined response $v_i(t)$ has been calculated by direct, time domain addition of

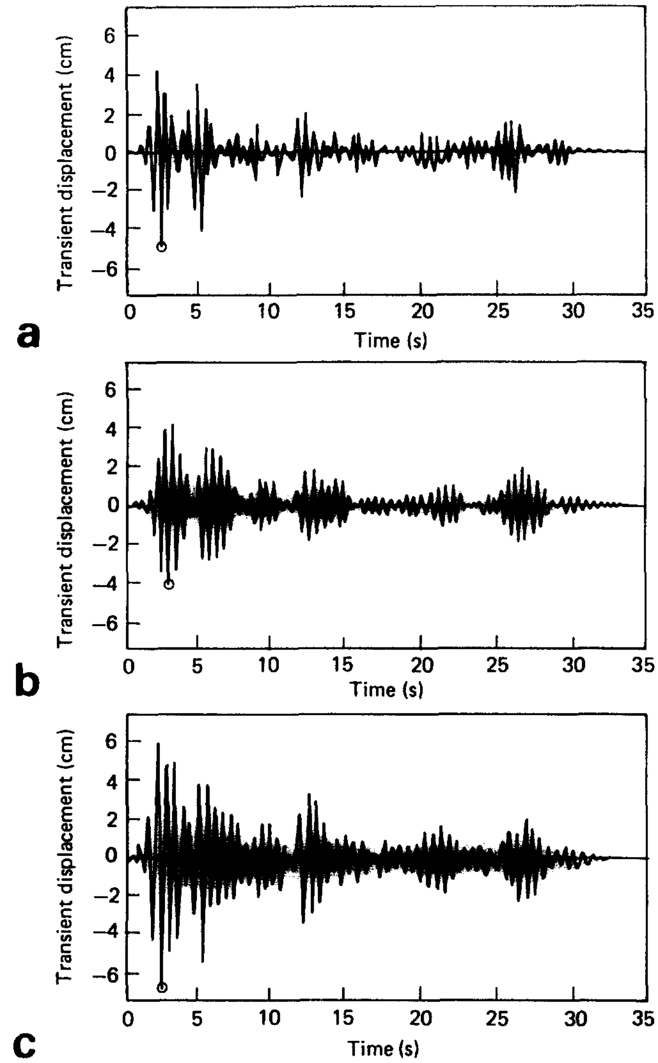

Figure 11 Transient displacement responses of torsionally coupled single storey building model subjected to N-S El Centro earthquake record: (a) translational, v; (b) torsional, v_θ; (c) combined, v_i; $e_r = 0.1$; $\lambda_T = 1$; $T_v = 0.5$ s; $\xi = 0.05$

the responses $v(t)$ and $v_\theta(t)$ and, hence, illustrates the importance of phasing in the calculation of the maximum combined response values, based only on a knowledge of the individual modal maxima. In this example, the computed maximum combined response (6.7 cm) compares favourably with the approximate square root of the sum of squares (SRSS) modal combination rule[17] commonly employed in response spectrum analyses. The SRSS value, based upon the maximum translational and torsional responses, in this case becomes:

$$(v_i)_{max} \simeq [(v)^2_{max} + (v_\theta)^2_{max}]^{\frac{1}{2}}$$
$$= [(5^2 + 4.1^2)]^{\frac{1}{2}} = 6.5\,\text{cm}$$

The SRSS value is, therefore, only 3% smaller than the computed maximum response value. Nevertheless, in general, care must be excercised when employing this combination technique in closely-coupled systems.[6] Whilst, in some circumstances, it can be useful to know the time history response pattern of a structure to an earthquake, as illustrated for example in *Figure 11*, the designer will in most cases be interested only in the values of the maximum responses, irrespective of the times at which they occur.

This philosophy has led to the widespread use of response spectra, a simple method which enables estimation of the individual modal maximum responses due to a particular earthquake, but which requires the specification of combination rules[17] to allow for the fact that these maxima do not necessarily occur simultaneously. In the response studies carried out in this present work, however, this problem is avoided since each individual response quantity is computed separately as a complete time history; the response maxima $(v)_{max}$ and $(v_\theta)_{max}$ are then selected from each record, as appropriate. The same is true of the combined response $v_i = v + v_\theta$ whose time history (the sum of the individual time histories v, v_θ) is computed prior to selecting the maximum response $(v_i)_{max}$.

The maximum displacement responses $(v)_{max}$, $(v_\theta)_{max}$ and $(v_i)_{max}$, normalized to the maximum ground displacement of the relevant earthquake records, are presented in *Figures 12–16*, where the responses to the European earthquake records are averaged under categories A and B. The uncoupled (translational) response curves are included in *Figures 12–16*, as appropriate, for purposes of comparison.

Figure 12 shows the displacement response curves for the El Centro earthquake for a system with $e_r = 0.15$ and for three selected values of λ_T. The translational response is generally reduced compared with the corresponding uncoupled values, especially for $\lambda_T = 1$, although the reduction is in most cases relatively small. As expected, the greatest torsional response occurs for $\lambda_T = 1$, except for periods longer than 1.1 s for which greatest response occurs for $\lambda_T > 1$. For $\lambda_T = 1$ the magnitude of the torsional response approaches, and occasionally exceeds, that of the corresponding translational response. The combined response, v_i, generally exceeds the corresponding uncoupled response values (translational only), and the amplification is especially significant in the longer period range with increases of edge displacement of up to 60%.

Since torsional coupling effects are, in general, most significant for $\lambda_T = 1$, this value is employed in plotting the remaining displacement response curves (*Figures 13–16*). *Figures 13–15* are plotted for a range of eccentricity ratios, and show the responses to the El Centro, European set A and European set B earthquakes, respectively. These graphs demonstrate the following response trends:

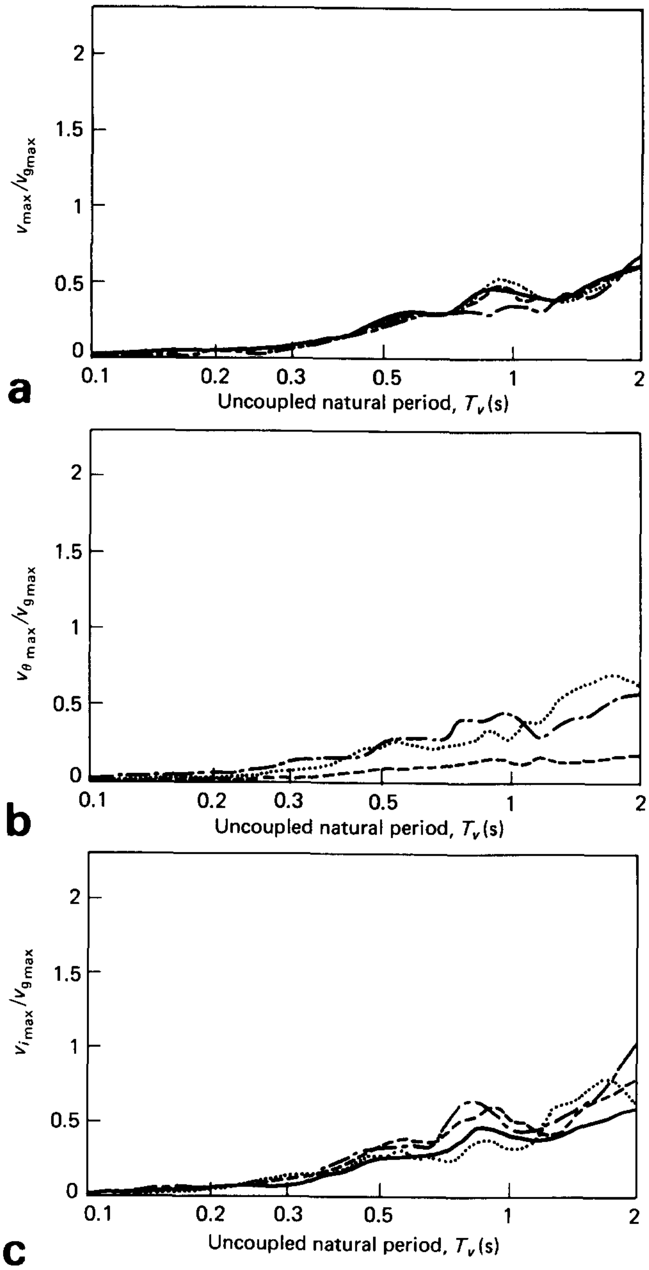

Figure 12 Normalized displacement response spectra for torsionally coupled building subjected to N–S El Centro earthquake record $e_r = 0.15$: (– – – –) $\lambda_T = 0.6$; (— – —) $\lambda_T = 1$; (····) $\lambda_T = 1.4$; (———) uncoupled; (a) translational; (b) torsional; (c) combined

- The reduction in translational response due to torsional coupling (that is, in comparison with the uncoupled response) is greater at large eccentricities. For $e_r = 0.3$, for example, the reduction may be of the order of 20–30%, depending on the value of T_v.
- The magnitude of the coupled torsional response increases with eccentricity, although the increase is not linear. An increase in eccentricity from $e_r = 0.05$ to $e_r = 0.15$ produces a twofold increase in torsional response. A further increase in eccentricity to $e_r =$

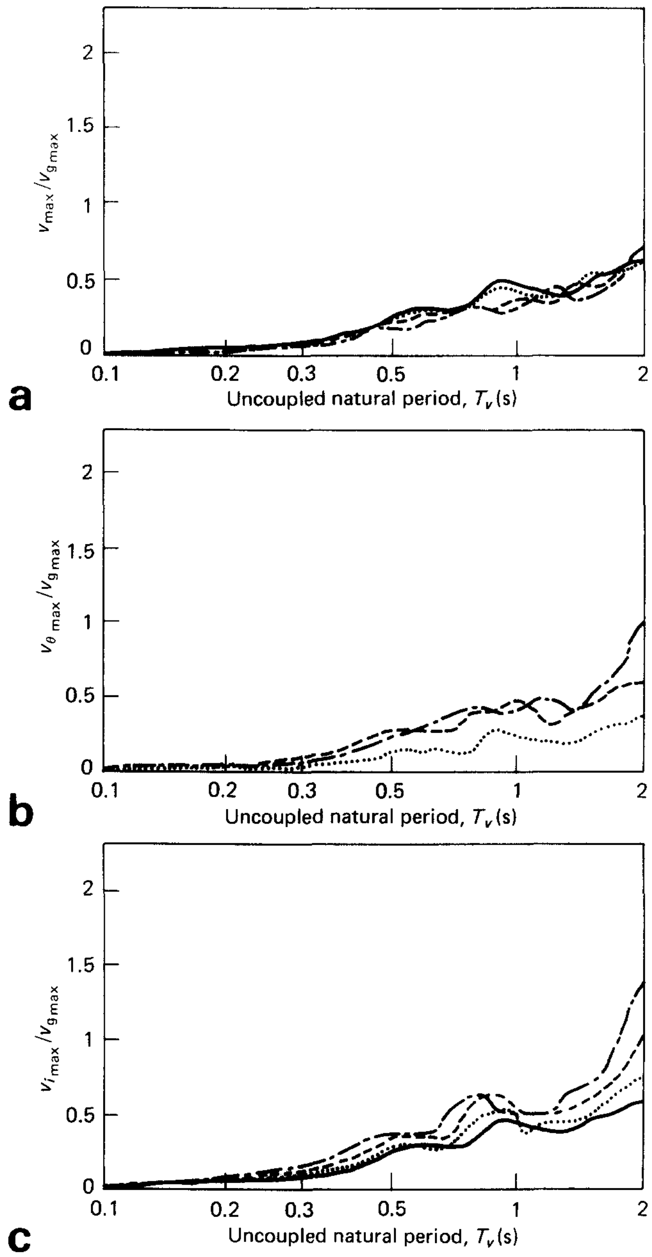

Figure 13 Normalized displacement response spectra for torsionally coupled building subjected to N–S El Centro earthquake record (λ_T = 1): (———) e_r = 0; (····) e_r = 0.05; (- - - -) e_r = 0.15; (— — —) e_r = 0.3; (a) translational; (b) torsional; (c) combined

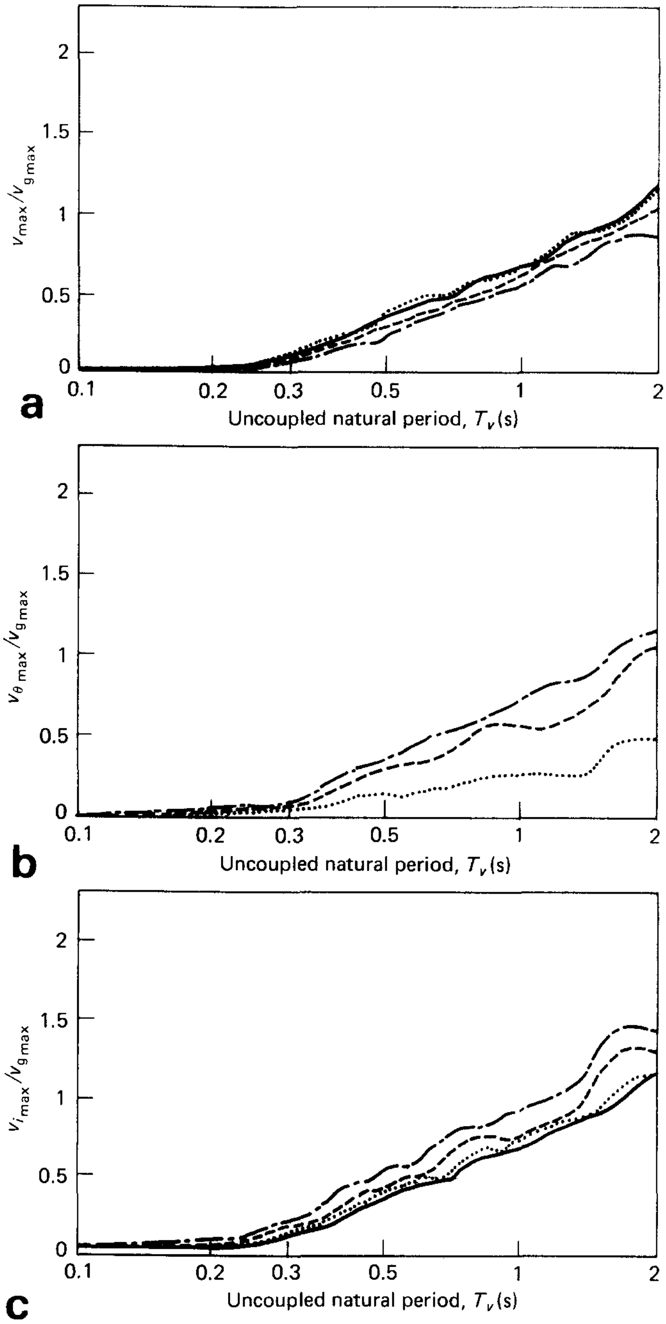

Figure 14 Normalized and averaged displacement response spectra for torsionally coupled building subjected to European set A earthquake records (λ_T = 1): (———) e_r = 0; (····) e_r = 0.05; (- - - -) e_r = 0.15; (— — —) e_r = 0.3; (a) translational; (b) torsional; (c) combined

0.3, produces a relatively smaller increase, by approximately 20% on average. It is concluded that at moderate to large eccentricities the effects of torsional coupling are less significant than at smaller eccentricities, an observation in accord with the earlier study of steady state responses.

- The magnitude of the torsional response, even for small eccentricity (e_r = 0.05), is significant compared with the translational response of the uncoupled system. For the El Centro earthquake (*Figure 13(b)*) the torsional response at this eccentricity is consistently greater than 50% of the uncoupled translational response, although for the European earthquakes the corresponding ratio is somewhat less. At large eccentricities (e_r = 0.3), the torsional response is generally greater than the corresponding uncoupled translational response by approximately 10–20%.
- The magnitude of the combined response, v_i, in all cases exceeds that of the uncoupled translational response, the amplification being greater at larger eccentricities. For the El Centro earthquake (*Figure 13(c)*), for example, the amplification in the longer period range for eccentricity e_r = 0.3 may exceed a factor of two compared with the uncoupled response. In contrast to the individual torsional response, the amplification of the combined response (in relation to uncoupled values) increases approximately linearly with eccentricity e_r.

For comparative purposes, the response curves for the El Centro, European set A and European set B earthquakes are shown in *Figure 16* for frequency and eccentricity ratios (λ_T and e_r) set to values of 1 and 0.15,

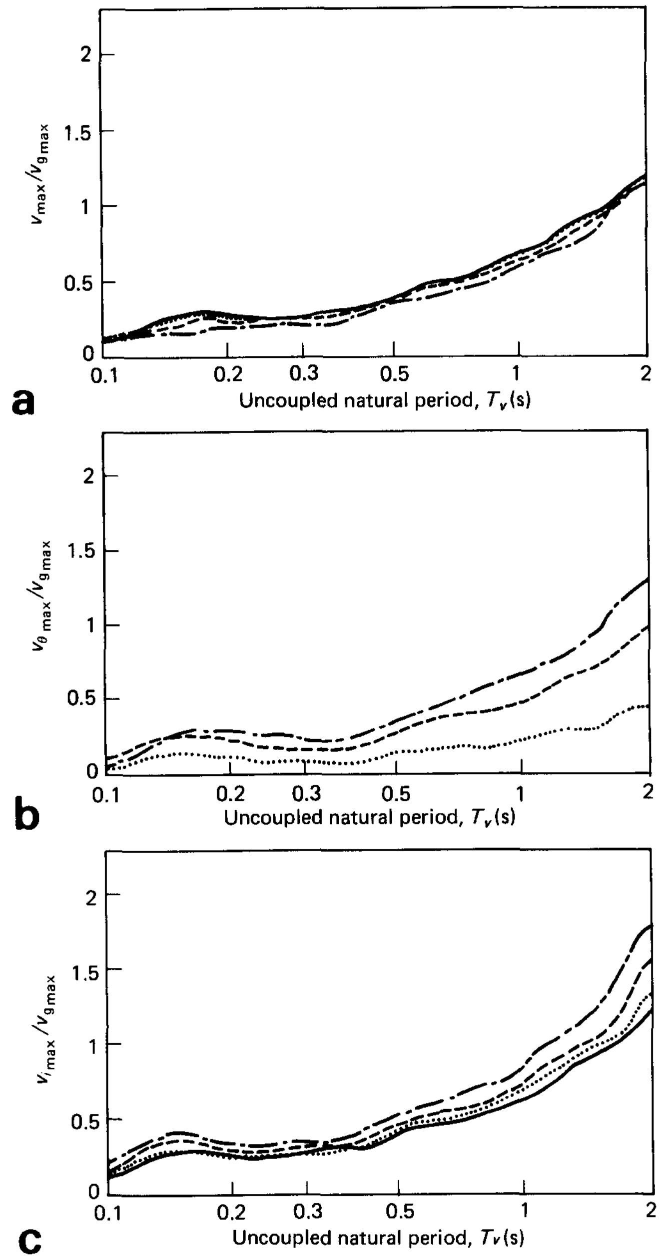

Figure 15 Normalized and averaged displacement response spectra for torsionally coupled building subjected to European set B earthquake records ($\lambda_T = 1$): (———) $e_r = 0$; (····) $e_r = 0.05$; (- - - -) $e_r = 0.15$; (— – —) $e_r = 0.3$; (a) translational; (b) torsional; (c) combined

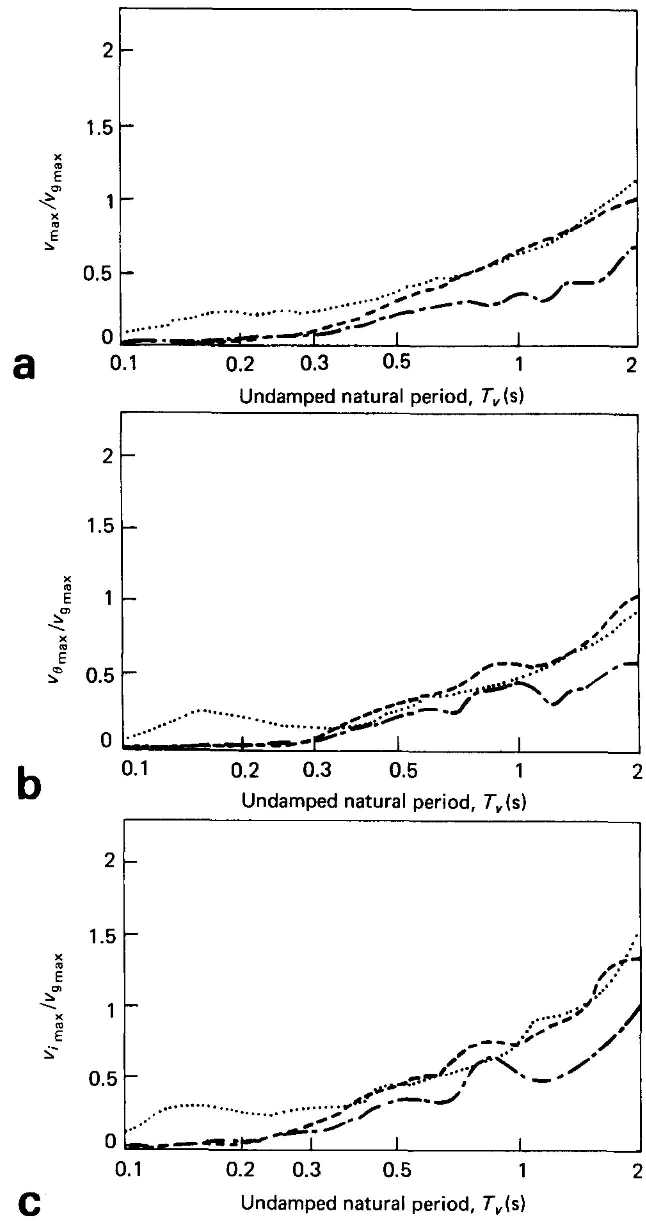

Figure 16 Normalized and averaged displacement response spectra for torsionally coupled building subjected to: (— – —) N–S El Centro; (- - - -) European set A; (····) European set B; $e_r = 0.15$; $\lambda_T = 1$; (a) translational; (b) torsional; (c) combined

respectively. The trends exhibited by the translational responses are identical to those of the corresponding uncoupled system, shown in earlier graphs, although relevant comparisons indicate a consistent reduction in response as a result of torsional coupling. The modal earthquake response trends have also been investigated in terms of maximum absolute acceleration responses, normalized to the peak ground acceleration. Selected results are shown in *Figures 17–19*, where the parameters e_r and λ_T for each figure correspond to those quoted for *Figures 12, 13* and *16*, respectively. The observed trends are identical, qualitatively, to those previously outlined for the displacement response curves.

Conclusions

Most analytical parametric studies of torsional coupling to date have employed idealized flat and hyperbolic response spectra to represent the earthquake input to the system.[5–9,23] Whilst this approach has considerable advantages over the more complex and costly time history techniques, it is nevertheless essential to assess and compare the observed response trends with those obtained when actual earthquake excitations are considered. The key purpose of this parametric study of the coupled lateral torsional responses of asymmetric buildings to steady state and earthquake base loadings has been to develop an understanding of the nature of torsional coupling. Based on the results presented, the following conclusions have been drawn:

- The most significant effects of torsional coupling are to produce a dynamic torque about the centre of resistance, together with a corresponding reduction in the dynamic shear force compared with the response of the related symmetric building. These effects are amplified when the uncoupled natural frequencies in

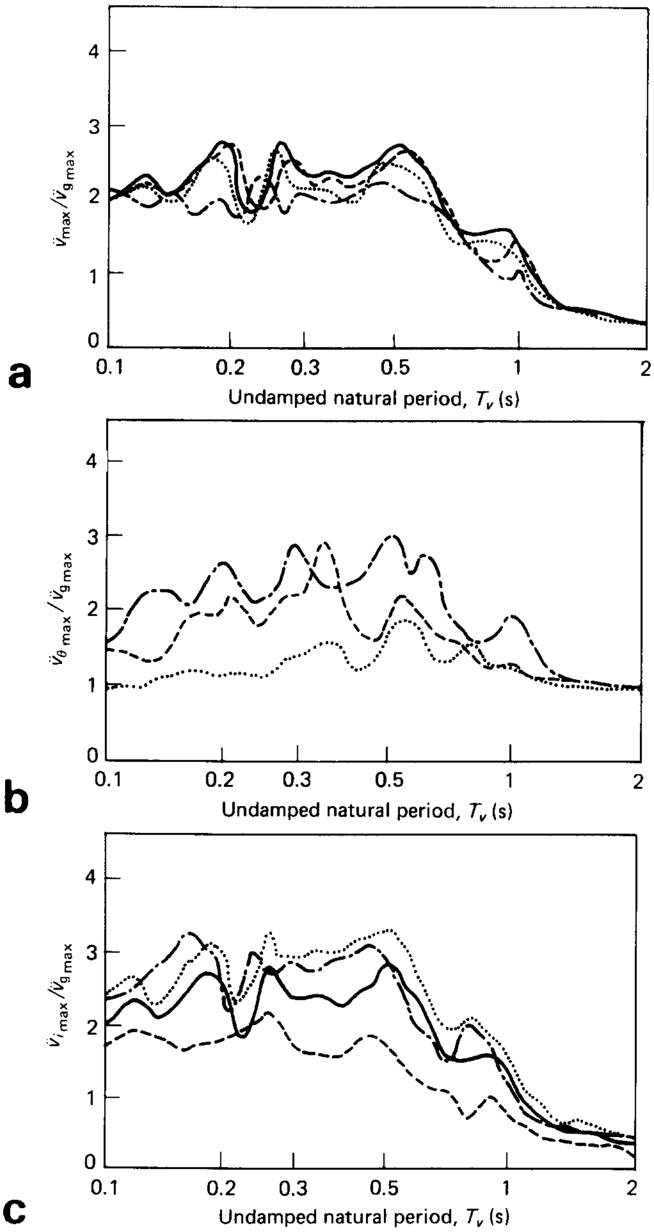

Figure 17 Normalized acceleration response spectra for torsionally coupled building subjected to N–S El Centro earthquake record (e_r = 0.15): (- - - -) λ_T = 0.6; (— — —) λ_T = 1; (····) λ_T = 1.4; (———) uncoupled; (a) translational; (b) torsional; (c) combined

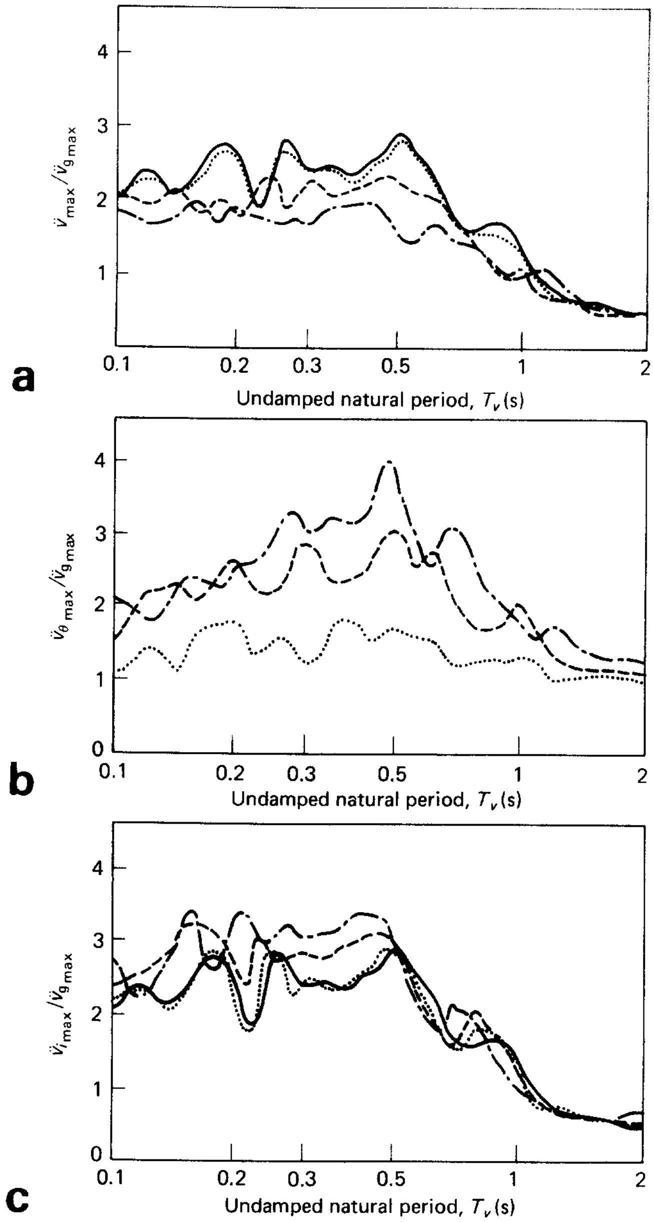

Figure 18 Normalized acceleration response spectra for torsionally coupled building subjected to N–S El Centro earthquake record (λ_T = 1): (———) e_r = 0; (····) e_r = 0.05; (- - - -) e_r = 0.15; (— — —) e_r = 0.3; (a) translational; (b) torsional; (c) combined

torsion and translation are close.

- Torsional response effects may be substantial even when the structural eccentricity is small. For e_r = 0.05, for example, the maximum displacement at the edge of the building due to the torsional component of response may exceed 50% of the corresponding maximum contribution from the translational component. Whilst torsional responses increase with the magnitude of the structural eccentricity, the nature of the effect is nonlinear with more rapid increases at small eccentricities.
- The combination of translational and torsional effects may result in significant increases in the lateral displacement of vertical members situated at the edge of the building. Under earthquake excitation, this increase may in some cases exceed 50% when the eccentricity is large.
- The effects specified in the three preceding paragraphs are not qualitatively affected by the nature of the base loading conditions. The calculation of average response effects for a number of earthquakes with similar spectral properties reveals a consistency in the trends of torsional coupling, even among records with widely differing frequency contents.
- A study of the influence of the controlling parameters e_r and λ_T of the structural system on earthquake response requires that a range of values of the uncoupled natural period T_v be considered in order to obtain reliable results.

Since many of the torsional design recommendations are based on the results of studies using idealized response spectra, it is clear that care is needed in extrapolating to systems subjected to actual ground excitation records. Further work in this area is required.

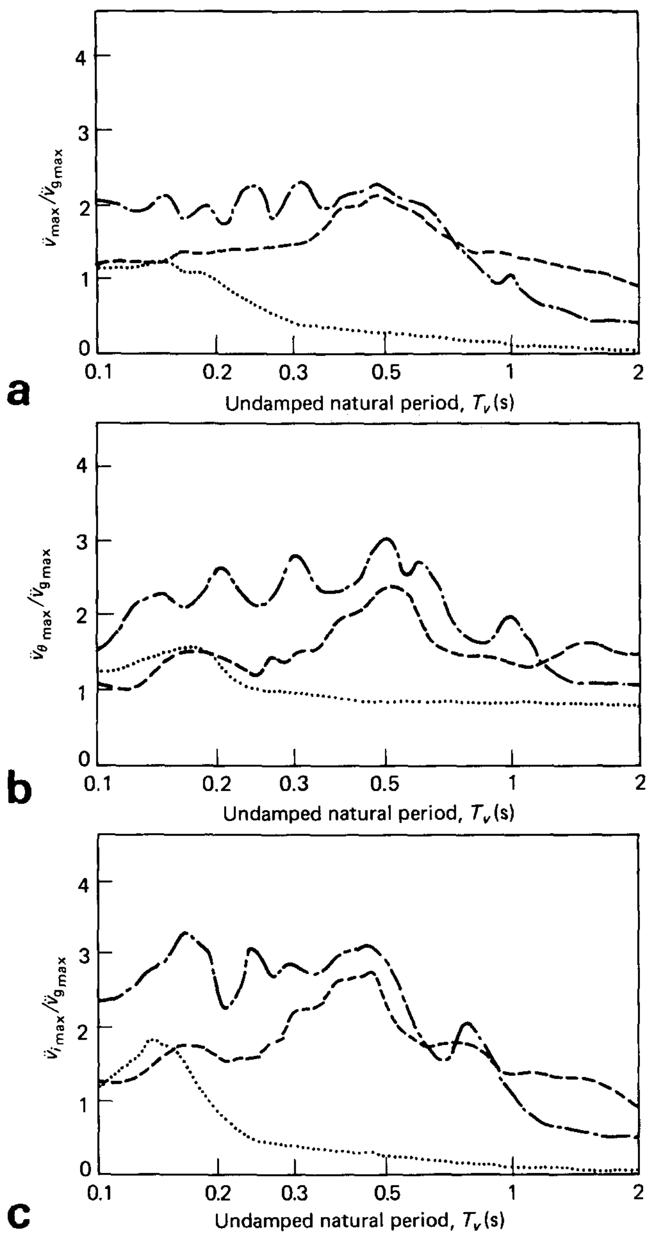

Figure 19 Normalized and averaged acceleration response spectra for torsionally coupled building subjected to: (— — —) N–S El Centro; (– – – –) European set A; (····) European set B; $e_r = 0.15$; $\lambda_T = 1$; (a) translational; (b) torsional; (c) combined

Nomenclature

$c_{vv}, c_{v\theta}, c_{\theta\theta}$	damping coefficients for structure
$D_{vv}, D_{v\theta}, D_{\theta\theta}$	dimensionless damping coefficients for structure
e	eccentricity between centres of mass and resistance
e_r	eccentricity ratio (e/r)
f	excitation frequency ratio (ω/ω_1)
i	imaginary unit ($[-1]^{\frac{1}{2}}$)
J_θ	mass polar moment of inertia of floor mass about z-axis
K_v	translational storey stiffness
K_θ	torsional storey stiffness
m	total mass of building
max	maximum value of response quantity
p_a, p_b	mass density of a and b parts of floor disc
r	radius of floor disc
t	time
T_v	uncoupled natural period of building ($=2\pi/\omega_v$)
$v, H_v, \bar{v}$	time history, complex frequency response and amplitude of translational displacement of floor disc
$v_\theta, H_\theta, \bar{v}_\theta$	time history, complex frequency response and amplitude of torsional displacement at periphery of floor disc
$v_i, H_i, \bar{v}_i$	time history, complex frequency response and amplitude of combined displacement at point i on edge of floor disc, distance r from x-axis
$v_g, \bar{v}_g$	time history and amplitude of translational displacement of ground
v^t	time history of total x-translational displacement of floor disc ($=v_g + v$)
x, y, z	Cartesian axes of reference x, y horizontal)
θ	rotation of floor disc about z-axis
ξ	modal ratio of critical damping
λ_T	uncoupled frequency ratio ($=\omega_\theta/\omega_v$)
π	3.14159265
$\psi_v, \psi_\theta, \psi_i$	phase angles for translational, torsional and combined responses of floor disc
ω	excitation frequency
ω_1, ω_2	fundamental and secondary natural frequencies of torsionally-coupled building
ω_v	translational natural frequency of torsionally uncoupled building
ω_θ	torsional natural frequency of torsionally uncoupled building
Ω_n	coupled natural frequency ratios (ω_n/ω_v; $n = 1,2$)

References

1 Foutch, D. A. 'The vibrational characteristics of a twelve-storey steel frame building', *Earthquake Eng. Struct. Dyn.*, 1978, **6** (3), 265–294

2 Jennings, P. C., Matthiesen, R. B. and Hoerner, J. B. 'Forced vibration of a tall steel frame building', *Earthquake Eng. Struct. Dyn.*, 1972, **1** (2), 107–132

3 Medearis, K. 'Coupled bending and torsional oscillations of a modern skyscraper', *Bull. Seism. Soc. Am.*, 1966, **56** (4), 937–946

4 Jennings, P. C. and Kuroiwa, J. H. 'Vibration and soil-structure interaction tests of a nine-storey reinforced concrete building', *Bull. Seism. Soc. Am.*, 1968, **58**, 891–916

5 Tsicnias, T. G. 'Coupled lateral and torsional earthquake response of buildings with rigid floor diaphragms', *Ph.D. Thesis*, University of London, 1981

6 Rosenblueth, E. and Elorduy, J. 'Responses of linear systems to certain transient disturbances', *Proc. 4th World Conf. Earthquake Eng.*, Santiago, Chile, 1969, **1** (A1), 185–196

7 Dempsey, K. M. and Irvine, H. M. 'Envelopes of maximum seismic response for a partially symmetric single-storey building model', *Earthquake Eng. Struct. Dyn.*, 1979, **7**, (2), 161–180

8 Kan, C. L. and Chopra, A. K. 'Effects of torsional coupling on earthquake forces in buildings', *J. Struct. Div. ASCE*, 1977, **103,** ST4, 805–819

9 Tso, W. K. and Dempsey, K. M. 'Seismic torsional provisions for dynamic eccentricity', *Earthquake Eng. Struct. Dyn.*, 1980, **8** (3), 275–289

10 Gluck, J., Reinhorn, A. and Rutenberg, A. 'Dynamic torsional coupling in tall building structures', *Proc. Inst. Civ. Eng.*, London, 1979, **67** (2), 411–424

11 Kan, C. L. and Chopra, A. K. 'Elastic earthquake analysis of torsionally coupled multi-storey buildings', *Earthquake Eng. Struct. Dyn.*, 1977, **5** (4), 395–412

12 Keintzel, E. 'On the seismic analysis of unsymmetrical single-storey buildings', *Proc. 5th World Conf. Earthquake Eng.*, Rome, 1973, 110–113

13 Elms, D. G. 'Seismic torsional effects on buildings', *Bull. NZ. Nat. Soc. Earthquake Eng.*, 1976, **9** (1), 79–83

14 Poole, R. A. 'Analysis for torsion employing provisions of NZRS 4203: 1974', *Bull. NZ. Nat. Soc. Earthquake Eng.*, 1977, **10** (4), 219–225

15 Rosenblueth, E. 'Seismic design requirements in a Mexican 1976 code', *Earthquake Eng. Struct. Dyn.*, 1979, **7** (1), 49–61

16 Muller, F. P. and Keintzel, E. 'Approximate analysis of torsional effects in the new German seismic code DIN 4149', *Proc. 6th Eur. Conf. Earthquake Eng.*, Dubrovnik, Yugoslavia, 1978, **2**, 101–108

17 Maison, B. F., Neuss, C. F. and Kasai, K. 'The comparative performance of seismic response spectrum combination rules in building analysis', *Earthquake Eng. Struct. Dyn.*, 1983, **11**, (5), 623–647

18 National Building Code of Canada, Associate Committee on the National Building Code, National Research Council of Canada, Ottawa, Ontario, 1985

19 Eurocode No. 8 'Common unified rules for structures in seismic regions', Commission of the European Communities (draft), 1984

20 Wong, H. L. and Trifunac, M. D. 'Generation of artificial strong motion accelerograms', *Earthquake Eng. Struct. Dyn.*, 1979, **7** (6), 509–527

21 Preumont, A. 'The generation of spectrum compatible accelerograms for the design of nuclear power plants', *Earthquake Eng. Struct. Dyn.*, 1984, **12**, (4), 481–497

22 Tsicnias, T. G. and Hutchinson, G. L. 'Evaluation of code requirements for the earthquake resistant design of torsionally coupled buildings', *Proc. Inst. Civ. Eng.*, London, 1981, **71** (2), 821–843

23 Dempsey, K. M. and Tso, W. K. 'An alternative path to seismic torsional provisions', *Soil Dyn. Earthquake Eng.*, 1982, **1** (1), 3–10

24 Hutchinson, G. L. and Tsicnias, T. G. 'Steady state effects of torsional coupling on rigidly and flexibly based buildings', *Rep. No. 82–01*, Department of Civil Engineering, King's College, London, 1982, 66p

25 Tso, W. K. and Meng, V. 'Torsional provisions in building codes', *Proc. 3rd Can. Conf. Earthquake Eng.*, Montreal, 1979, **1**, 663–684

26 Wang, P. C. and Yun, C. B. 'Site-dependent critical design spectra', *Earthquake Eng. Struct. Dyn.*, 1979, **7**, (6), 569–578

27 Hutchinson, G. L. and Navidi, A. 'Evaluation of earthquake response of low-rise structures using design codes and local specifications', *Bull. NZ. Nat. Soc. Earthquake Eng.*, 1983, **16** (4), 331–344

28 Brady, A. G. 'Studies of response to earthquake ground motion', Earthquake Engineering Research Institute, California Institute of Technology, California, 1968

29 Chandler, A. M. 'Coupled torsional response of single-storey building models to earthquake loading', *Ph.D. Thesis*, University of London, 1985

30 Tezcan, S. S., Yerlici, V. and Durgunoglu, H. T. . 'A reconnaissance report for the Romanian earthquake of 4 March 1977', *Earthquake Eng. Struct. Dyn.*, 1978, **6** (4), 397–421

31 Chandler, A. M. and Hutchinson, G. L. 'Discrete and fast Fourier transforms as applied to earthquake engineering', *Rep. No. 83–03*, Department of Civil Engineering, King's College, London, 1983, 229p

32 Hall, J. F. 'An FFT algorithm for structural dynamics', *Earthquake Eng. Struct. Dyn.*, 1982, **10**, (6), 797–811